Heliyon 9 (2023) e19996

Contents lists available at ScienceDirect

Heliyon

journal homepage: www.cell.com/heliyon

Phosphorus recovery from agricultural waste via cactus pear biomass

Nicolò Auteri *, Riccardo Scalenghe, Filippo Saiano

Dipartimento Scienze Agrarie, Alimentari e Forestali, Università degli Studi di Palermo, Italy

ARTICLE INFO

Keywords:
Adsorption
Desorption
Opuntia ficus-indica
Agricultural waste
Circular economy

ABSTRACT

In this study, the potential of cactus pear pruning waste (CPPW) as a low-cost adsorbent biomass for phosphorus (P) removal from aqueous solutions was investigated in batch mode. Biomass samples derived from cactus pear were collected and analyzed to investigate their properties when enriched with either calcium (Ca) or iron (Fe). The examination focused on the capacity of these samples to remove P. The P removal capacities were determined to be 2.27 mg g^{-1}, 1.33 mg g^{-1}, and 1.87 mg g^{-1} for Ca^{2+}-enriched, Fe^{2+}-loaded, and Fe^{3+}-loaded biomass respectively. Among the various models studied, the Langmuir isotherm model was identified as the most appropriate for accurately describing the P adsorption the enriched biomass. The kinetics of the adsorption process were analyzed by applying the pseudo-first-order, pseudo-second-order, and intraparticle diffusion models. The pseudo-second-order model provided the best fit to the experimental data. Furthermore, the desorption and regeneration process was investigated, revealing minimal P desorption (less than 8%) from Ca or Fe-loaded biomass, indicating the strong stability of the biomass-cation-P system.

The estimated cost ranged from 8 to 161 euros per tonne, with an additional 230 euros when considering the pruning costs inherent to the crop. These costs fall below the threshold (320 euros per tonne) for the economically viable P reuse at the farm level. Consequently, CPPW, when reduced to powder and loaded with ions, emerges as an affordable adsorbent with good removal performance, offering a promising avenue for direct utilization in agriculture as both soil conditioner and fertiliser.

1. Introduction

Phosphorus (P) is an indispensable element that is fundamental for the existence of life that ensures the global food supply is adequately produced [1]. Global P extraction will peak in the coming decades, leading to impacts on food security [2]. Phosphorus is also a key nutrient that ensures soil fertility and is an important source of eutrophication [3,4]. Thus, there is a growing interest in methodologies to remove P from water bodies, particularly through the use of natural or waste materials, which fits within a sustainable cycle of P recovery. In recent years, researchers have proposed environmentally friendly and cost-effective adsorbents derived from agricultural waste materials which can be utilized for sustainable P recovery, with or without further modification. These approaches aim to maximize the utility of waste materials while ensuring sustainable P management [5]. Numerous studies have explored the capacity of various biomass adsorbents, including corn bracts [6,7], sugar cane bagasse [8] and wheat straw [9], dried

* Corresponding author.
E-mail address: nicolo.auteri@unipa.it (N. Auteri).

https://doi.org/10.1016/j.heliyon.2023.e19996
Received 16 June 2023; Received in revised form 7 September 2023; Accepted 7 September 2023
Available online 12 September 2023

cactus pear pruning [10,11]. Currently, cactus pear thrives in semi-arid regions across the globe and finds significant cultivation in the Mediterranean basin and Central America. Annual pruning results in the disposal of 13–15 tons ha^{-1} of biomass [12]. This plant produces a hydrocolloid, known as 'mucilage', which has the ability to form a network trapping large amount of water. Opuntias are grown across 3 million hectares of small farms; their resilience in arid climates renders cactus pear essential for food security. It finds applications in agro-forestry systems, where it can be intercropped with legumes and annual crops. Contributing to the circular economy of agricultural production, even on a local scale, can have a widespread impact throughout the world, as it helps to mitigate the overall environmental impact. This already serves as a beneficial purpose.

The present study explores the capability of dried cactus pear as an environmentally friendly P adsorbent from water. The study's main objective is to investigate P adsorption by untreated and chemically modified pruning waste (cladodes) of cactus pear. Chemical modification, such as enriching with Ca^{2+} or Fe (Fe^{2+}, Fe^{3+}) elements, wherein positive charges are exclusively attributed to calcium (Ca) exhibiting a bivalent charge, and iron (Fe) demonstrating both bivalent and trivalent charges within the biomass's chemical composition, is expected to enhance P removal. The research objective was to delineate the operational parameters for employing biomass in the recovery of P from water and its subsequent release into the rhizosphere. Critical concentrations, timings, and chemical factors (particularly pH and ionic charges) were measured to propose feasible application scenarios.

2. Materials and methods

2.1. Cultivation waste

Cladodes from cactus pear (*Opuntia ficus-indica* (L.) Mill. *cv* Gialla) were collected during the fall season in Roccamena (IT) (37°50′17″88 N, 13°9′20″16 E; 472 m a.s.l.). We collected cladodes which would be removed in normal annual pruning (Fig. 1*a*). The spines were removed with a knife after harvesting, after being washed with tap water and then with deionized water, were air-dried, manually dissected (average handling time ≈ 35 min kg^{-1} cladode), dried (48 h, 105 °C) (Fig. 1*b–c*). The dried cladodes underwent grinding using a laboratory blender (Fig. 1*d*) and were subsequently sieved into various size fractions, $Ø \leq 0.250$ mm; $0.250 \text{ mm} < Ø \leq 2$ mm; $Ø > 2$ mm, and stored at room temperature. Subsequently, we will refer to this material as 'biomass' for the sake of brevity.

2.2. Material characterization

2.2.1. Lewis basic sites determination

Data regarding the quantity of Lewis basic sites present on the biomass was acquired and employed as a reference for conducting

Fig. 1. Cactus pear, *Opuntia ficus-indica* (L.) Mill.: a) the cactus pear production chain is, at the European level, exclusive to Sicily which holds the monopoly of the Italian market and over 90% of the EU market. The total area involved in the cultivation of cactus pear in Sicily is about 4000 ha. The most important area in terms of surface and degree of specialization of the plants are the areas of San Cono (37°17′24″N, 14°22′02″E), Santa Margherita Belice (37°41′34″N, 13°01′16″E) and Roccapalumba (37°48′01″N, 13°38′02″E); b) cladodes *cv* Gialla 2 years old; c) cladodes manually dissected; d) biomass.

adsorption studies, facilitating the assessment of the experimental molar ratio in relation to metal ions [13]. In brief, a suspension of 5 g of biomass was treated in 0.1 M KOH solution, and then in 30 mL of 0.5 M HCl solution. Subsequently, the mixture was stirred for 24 h. After this duration, 5 mL of filtered solution (0.45 μm) was extracted and titrated with 0.1 M NaOH solution. The differences in hydrogen ion (H^+) quantities within the solution of the biomass provide the basic Lewis site equivalents.

2.2.2. Treatments of biomass

The biomass treatments were carried out with the addition of metal ions, which could improve the ability of biomass for P uptake. These ions were chosen for their non-toxic and environmentally friendly characteristics when used as soil conditioners or fertilizers. Due to these considerations, we opted for Ca and Fe ions. Initially, we added 5 g of biomass directly in 50 mL of a solution containing 50 mmol of $Ca(OH)_2$, and the mixture was shaken for 24 h. Further attempts were made were made to introduce more Ca ions into the biomass's chemical composition. This was achieved by treating 5 g of the biomass with 50 mL of solution with 10 mmol of KOH for 24 h, followed sequentially by 50 mmol of $CaCl_2$ for another 24 h.

For comparison, we aimed to enhance the P adsorption capacity of the biomass using Fe ions. In the first attempt, 5 g of biomass was directly exposed to 50 mL, both with 50 mmol of $FeSO_4$ (with ferrous iron) and 50 mmol of $FeCl_3$ (with ferric iron) and the mixture was shaken for 24 h. Similar to the Ca treatment, we treated 5 g of biomass with 10 mmol of KOH for 24 h and, successively, with both 50 mL of a solution containing 50 mmol of $FeSO_4$ and 50 mL of a solution containing 50 mmol of $FeCl_3$. The mixtures were shaken for 24 h. After treating the biomass with these three cations, the solid residue was separated from the solvent by centrifugation (7000 rpm for 10 min) and rinsed with ultrapure water two times. Subsequently, the solids were then placed in an oven at 105 °C for 24 h.

The initial P content of the biomass used for the experiments was measured by mineralization of the sample and determination of the P content with UV–Vis spectrophotometry. On the treated materials, release tests of Ca^{2+}, Fe^{+2} and Fe^{3+} in ultrapure water, to verify the stability of the chemical interaction between the biomass and cations, were performed by immersing 1 g of the treated biomass in 30 mL of ultrapure water for 24 h. All tests were performed in duplicate.

Together with Fe and Ca, the content of Zn, Cu, Cd, Ni, Pb, Mn and Cr, on the biomass was determined. Metal content analyses were conducted using an Agilent ICP-MS 7500ce instrument operating in quantitative mode, employing an external calibration method in the range of 50–5000 ng mL^{-1}, and with ^{103}Rh, 1000 ng mL^{-1}, as internal standard. Three replicates were always performed. The attainment of all solutions involved the process of diluting the respective ICP grade standard (1000 ng mL^{-1}).

Numerous approaches exist for repurposing this biomass within agricultural settings. The most suitable approach for a given farm will hinge on various factors, including waste quantity, waste quality, space availability, equipment access, and budget considerations. Potential reusing methods encompass chopping, drying, and ionic treatment. Drying serves to reduce the volume facilitating storage. Ionic treatment, involving the loading of Ca or Fe ions necessitates the presence of cost-free sources of these ions on the farm, such as rocks or ferrous waste. The specifics of each method may differ based on the chosen approach. However, the general process is as follows: (i) reduce the size of the pruning waste by chipping, shredding, or baling (drying, if necessary, only), (ii) loading with ions, and (iii) apply the treated material. With this material ready, the P adsorption choices depend on where it must be recycled (irrigation channels, drains, watercourses), the filter system must be implemented on a case-by-case basis. The criterion is the optimization of the loading and unloading times of the immersion chambers. The final phase, after being enriched in P, is the use. In the case of small volumes, e.g., used in horticulture, after drying, the material can be bagged and stored. In the case of large volumes, the undried material can be distributed in the open field with manure spreaders. The pivotal determinant for success rests upon selecting the appropriate approach tailored to the specific farm's needs.

2.2.3. Infrared spectroscopy (FT-IR)

To gain a comprehensive understanding of its potential as P adsorbent, we subjected both the chemically treated biomass with Ca^{2+}, Fe^{+2} and Fe^{3+}, and the untreated biomass using the Fourier-transform infrared spectroscopy (FT-IR). We followed the methodology outlined by Barbera et al. [14] albeit with a primary focus on evaluating the functional groups responsible for the interaction between the biomass and phosphate ions. Spectra are in the range 4000–400 cm^{-1} obtained by a PerkinElmer FT-IR spectrometer Spectrum Two. A total of 64 scans were acquired for each spectrum recorded at a resolution of 4 cm^{-1}. The acquisition and manipulation of spectra were made possible through the utilization of the PerkinElmer software.

2.2.4. Point zero charges (PZC)

We conducted electrophoretic mobility measurements using on the Doppler velocimetry technique [15]. Electrophoretic mobility was determined by analyzing the frequency shift between the incident and scattered light measurements. Zeta potential was then derived from the electrophoretic mobility using a numerical approximate solution [16]. To calculate the kinetic zero charge (PZC) value of the particles, the solid addition method was employed. For this, we employed six different vials containing solutions of HCl and NaOH in various proportions. This was done to adjust the initial pH values within the range of 3.5–9.0. Approximately 0.300 μg of the biomass was added to 20 mL of ultrapure water and shaken on an orbital platform shaker at 300 rpm for 24 h. From the resulting suspension, 0.200 mL was drawn and mixed with 2.5 mL of ultrapure water at the chosen pH. The mixture was resuspended for 12 h, reaching a the final volume of 5 mL. Subsequently, the Z potential (mV) was measured using a Coulter DELSA 440 SX instrument. The pH values against the corresponding mV values were plotted, from which the PZC was determined.

2.3. Batch adsorption and desorption

Two solutions containing approximately 1 mmol with, respectively, hydrogen phosphate and dihydrogen phosphate ions in

ultrapure water, were prepared. These were chosen because they are the principal inorganic phosphate species present in a range of pH between 5 and 8, typical of freshwater runoff.

Adsorption batch experiments, conducted at room temperature (≈22 °C). In each setup, 1.5 g of both biomass types were immersed in 50 mL of phosphate solutions, which were stirred together (250 rpm) overnight. Then, the adsorbent matrix was separated by centrifugation at 7000 rpm for 10 min, and the concentration of phosphate ions in the solution was determined by UV–Vis spectrophotometry. All experiments were performed in triplicate. For the adsorption test, various sizes of the biomass matrix were used. Notably, there was no significant difference observed in the P adsorption phenomenon across the different particle sizes. The pH of the KH_2PO_4 solution initially started at a value of 5.1. After being in contact with the untreated biomass, it increased to pH 5.7 after 1 h, then gradually decreased and stabilized to pH 5.3 after 24 h. Similarly, the pH of the K_2HPO_4 solution began at pH 8.8. Upon contact with the biomass, it gradually decreased to a sub-acidic pH stabilizing at pH 5.3. The pH of both solutions in contact with the biomass attained a stable value in both cases at a sub-acidic pH of around 5.5, the same pH measured by immersing the biomass in ultrapure water, both after 1 h and 24 h. Regarding the pH values from the contact of the chemically modified biomasses with the phosphate solutions in K_2HPO_4 and KH_2PO_4, they are both 5.8 ± 0.1 after 24 h. Notably, the varied particle sizes of the biomass do not affect the pH of the solutions (data not shown).

Desorption tests were carried out on biomass enriched in Ca and Fe by immersing 1 g of treated biomass in 30 mL of ultrapure water for 24 h to evaluate the Ca and Fe content stably bound to the biomass. The same experimental conditions were repeated to assess P desorption from the biomass previously used for the P adsorption tests.

2.4. Modelling

2.4.1. Kinetic modelling

The contact time selected for the adsorption experiments were 1 and 24 h. To delve into the kinetics of adsorption, further contact times were 15, 30, 45, 60 min, as well as 5 and 24 h.

The gathered experimental data was subjected to analysis using both pseudo-first-order and pseudo-second-order kinetic models. Additionally, intraparticle diffusion was considered to examine the controlling mechanism involved in the biosorption of ions onto biomass. This encompassed aspects of mass transfer and chemical reactions.

The pseudo-first-order equation [1] follows the Lagergren theory of adsorption of soluble substances, and is given as:

$$q_t = q_{eq}\left(1 - e_1^{-k^t}\right) \quad [1]$$

where q_{eq} and q_t are the amounts in mg g^{-1} of adsorbed ions on the biomass at equilibrium at time t and k_1 is the first-order biosorption rate constant in min^{-1}.

The pseudo-second-order equation [2] is also based on the sorption capacity of the solid phase and is given as [17]:

$$q_t = q_{eq}^2\, k_2\, t \Big/ (1 + k_2 q_e t) \quad [2]$$

where k_2 is the second-order biosorption rate constant (g mg^{-1} min^{-1}), and q_{eq} is the biosorption capacity at the equilibrium (mg g^{-1}).

When intraparticle diffusion is the rate-limiting step, the adsorbate uptake varies with the square root of time. The intraparticle equation [3] can be described as [18]:

$$q_t = K_s t^{0.5} \quad [3]$$

where q_t is the amount of adsorbed ions at the contact time t (min) and K_s is the intraparticle diffusion constant.

2.4.1.1. Equilibrium isotherm models. The adsorption isotherm data for P onto the biomass, in both single and multi-component system, were analyzed using both Langmuir and Freundlich equations. The Langmuir model [4], monolayer sorption of a solute from a solution, is given by

$$q_{eq} = Q_{max} k_1 C_{eq}\left(1 + k_1 C_{eq}\right)^{-1} \quad [4]$$

where.

q_{eq} = equilibrium adsorbate loading on the biomass (mg adsorbate g^{-1} of biomass);
C_{eq} = equilibrium concentration of the adsorbate (mg adsorbate L^{-1});
Q_{max} = ultimate capacity (mg adsorbate g^{-1} of biomass);
k_1 = relative energy (intensity) of adsorption (L mg^{-1}), also known as binding constant.

The Freundlich model [5], based on sorption on a heterogeneous surface, is represented as

$$q_{eq} = K_2 C_{eq}^{1/n} \quad [5]$$

where.

q_{eq} = equilibrium adsorbate loading on the biomass (mg adsorbate g^{-1} of biomass);
C_{eq} = equilibrium concentration of the adsorbate (mg adsorbate L^{-1}

K_2 = Freundlich adsorption constant
n = Freundlich exponent.

K_f and n are the Freundlich constants indicative of adsorption capacity and adsorption intensity, respectively. Values of n between 1 and 10 are favourable for adsorption.

3. Results

3.1. Biomass characterization

3.1.1. Lewis basic sites

Lewis basic sites on our biomass measured 2.31 ± 0.08 mmol H^+g^{-1}. The significance of these values lies in their ability to determine the maximum amount of calcium and iron that, when added to biomass, can influence the absorption of dissolved phosphate ions within the solution. For bivalent (Ca^{2+}, Fe^{2+}) or trivalent cations (Fe^{3+}), the respective maximum adsorption capacity were found to be 1.16 ± 0.04 and 0.77 ± 0.03 mmol g^{-1}, respectively.

3.1.2. Point of zero charge

The pH value at which the functional groups of the adsorbent surface do not influence the pH of the solution during adsorption is the pH at the PZC. Based on the zeta-potential measurements conducted on our biomass, both enriched and non-enriched, in water, it has been determined that the PZC falls within the pH range of 5.5–5.8. Consequently, when the pH value was lower than the pH at PZC, the surface charge of the enriched biomass was found to be slightly negative. For pH values higher than the pH at PZC the surface charge of the modified biomasses was found highly negative.

3.1.3. Calcium and iron on natural and treated biomass

The Ca and Fe content in the chemical composition of the cladode, obtained through the mineralization of the solid material and subsequent measurement, was about 57.5 mg Ca and 4.6 mg Fe per 1 g of biomass. The attempt to enrich the biomass using $Ca(OH)_2$ increased the Ca content to 166.6 mg g^{-1}. In the second treatment, a significant increase in Ca content of 184.0 mg g^{-1} was observed (Table 1). Similarly, when using Fe ions, the attempt using directly both $FeSO_4$ and $FeCl_3$, obtained 9.7 and 7.1 mg Fe g^{-1} of cladode powder, respectively. In the second attempt, the Fe content increased significantly and 60.8 and 103.1 mg Fe g^{-1} for Fe^{2+} and Fe^{3+} respectively were measured (Table 1). All these materials (biomass + Ca^{2+}; biomass + KOH + Ca^{2+}; biomass + Fe^{2+}; biomass + Fe^{3+}; biomass + KOH + Fe^{2+}; biomass + KOH + Fe^{3+}) subsequently employed in batch P adsorption tests. The initial biomass used had a P content of 0.45 mg P g^{-1}. The chemical composition of the biomass, obtained from the mineralization of the solid material and subsequent measurement values, revealed low levels of Zn, Cd, Cu, Ni, Pb, Mn and Cr expressed in μg/g (as provided in Supplementary Material). These levels were consistently below the contamination threshold concentrations of contamination established for soils in agricultural areas (EC Regulation 1907/2006 and EPA540/R-96/018).

3.1.4. FT-IR spectra

The FT-IR spectral analysis (Fig. 2) reveals various absorption peaks, each corresponding to specific molecular vibrations [14, 19–21]. Within the range of 3700–2500 cm^{-1}, a broad absorption band is observed, indicating the intramolecular vibrational stretching of the –OH groups, which are extensively engaged in hydrogen bonding. Furthermore, weak peaks at 2842 and 2932 cm^{-1} can be attributed to the symmetric and asymmetric stretching vibrations of the C–H bonds in the CH_3 and CH_2 groups, respectively [22]. Transitioning below 2000 cm^{-1}, a series of broad bands between 1730 and 1500 cm^{-1} become evident. Among these, a medium-intensity shoulder at 1720 cm^{-1} is indicative of the C═O stretching of non-ionized carboxylic acid groups or other carbonyl-containing compounds. The bands observed at 1645, 1618, and 1520 cm^{-1} can be attributed to the vibrations of amide I, amide II, and C═C bonds, as well as the asymmetric stretching of the –COO– group. Moreover, bending vibrations of –OH and –CH in the $–CH_2$ groups are evident at 1634 cm^{-1} and 1427 cm^{-1}, respectively. In the range between 1480 and 1300 cm^{-1}, the absorption peaks are associated with the C–H bending vibrations of the CH_3 and CH_2 groups, in addition to the symmetric stretching of –COO– and stretching of the C–N group. Vibrational peaks at 1241 cm^{-1} indicate C–*O*–H bending, while peaks at 1143 cm^{-1} correspond to the

Table 1
Ca and Fe (mg g^{-1}) content in biomass after Ca or Fe enrichment.

Treatment	Ca content biomass (mg g^{-1})		Fe content biomass (mg g^{-1})	
		dev. std.		*dev. std.*
non-treated	57.5	*17.9*	4.3	*1.6*
$Ca(OH)_2$	166.6	*2.2*		
$FeSO_4$			9.7	*1.8*
$FeCl_3$			7.1	*0.7*
KOH + $CaCl_2$ (10 mmol)	125.9	*2.7*		
KOH + $CaCl_2$ (50 mmol)	184.0	*1.2*		
KOH + $FeSO_4$			60.8	*8.2*
KOH + $FeCl_3$			103.1	*32.4*

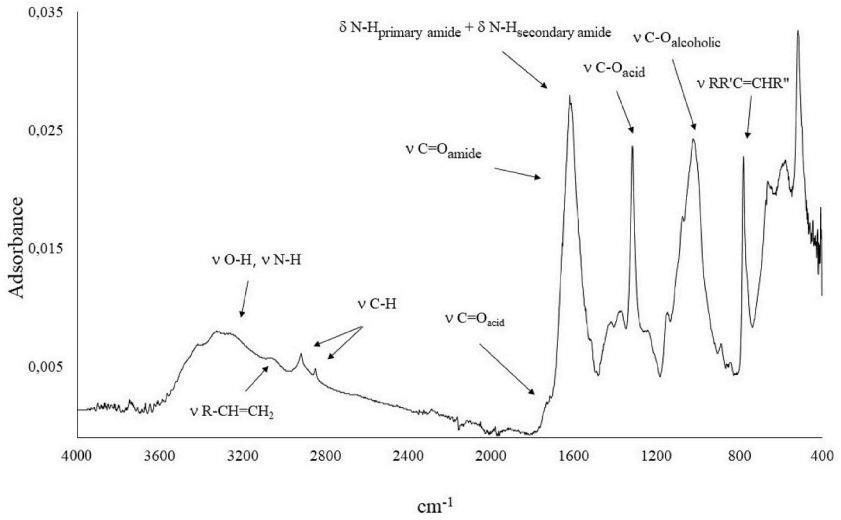

Fig. 2. FT-IR spectra of *Opuntia ficus-indica* dry biomass. The functional groups present in the biomass have been evaluated. Some of them may be involved in the interaction between biomass and phosphate ions.

asymmetric stretching of the C–*O*–C glucosidic bond. Between 1180 and 950 cm^{-1}, the observed bands are related to the C–OH and C–*O*–C groups of alcohols or ethers. Finally, the bands at 888 and 780 cm^{-1} can be attributed to the out-of-plane deformation of C–H groups in compounds of the RR'C═CHR″ type or similar structures. Notably, in the treated biomass samples, no new signals were observed by FT-IR spectra (data not shown). Normally, phosphate ions exhibit characteristic peaks within the range of 1000–1100 cm^{-1} [23]. However, in our particulat case, the presence of broad and intense bands between 1180 and 950 cm^{-1}, associated with the C–OH and C–*O*–C groups typically found in alcohols or ethers, masks the distinctive features of the phosphate ions.

3.2. Batch adsorption performances

The experimental results of the pure biomass, irrespective of the use of any of the three different particle sizes, revealed no significant chemical interaction of adsorbent with the different phosphate anions. Phosphorus adsorption tests conducted with the solution containing $H_2PO_4^-$ ions did not yield positive outcomes: both the biomass, whether Ca-enriched or not, exhibited limited ability to remove $H_2PO_4^-$ ions present in the solution. More precisely, the adsorption was only 5%, after 1 h with Ca-enriched biomass, with particle size 0.250 mm $< Ø \leq$ 2 mm. However, the sorbed P, within 24 h, was subsequently released back into the solution, highlighting a lack of meaningful adsorption capacity. The batch experiments conducted using a solution containing HPO_4^{2-} ions yielded different results: a removal capacity of about 46% was measured after 1 h, which then stabilized at 43% after 24 h (Table 2). This behaviour was consistent across all sizes of biomass. Notably, even after 24 h, the P removal capacity of the three particle sizes remained nearly unchanged. No substantial difference was observed in the P adsorption phenomena, using different particle sizes. As a result, the intermediate particle size (0.250 μm $< Ø \leq$ 2 mm), was selected for the subsequent experiments.

Table 2
P adsorption of Ca-enriched biomass, after 1 and 24 h, in $H_2PO_4^-$ and HPO_4^{2-} solutions.

$H_2PO_4^-$ solution						
Samples	Ø	C_0 mg P 50 mL	$C_{(1h)}$ mg P g^{-1}	P $_{(1h)}$ removal	$C_{(24h)}$ mg P g^{-1}	P $_{(24h)}$ removal
Ca-biomass	2 mm	5.1	<0.1	2%	<0.1	3%
dev. std.			-		-	
Ca-biomass	>250 μm		0.3	5%	<0.1	0%
dev. std.			*0.2*		-	
Ca-biomass	<250 μm		0.3	6%	<0.1	0%
dev. std.			*0.1*		-	
HPO_4^{2-} solution						
Samples	Ø	C_0 mg P 50 mL	$C_{(1h)}$ mg P g^{-1}	P $_{(1h)}$ removal	$C_{(24h)}$ mg P g^{-1}	P $_{(24h)}$ removal
Ca-biomass	2 mm	4.8	2.0	42%	1.9	40%
dev. std.			*0.1*		*0.2*	
Ca-biomass	>250 μm		2.2	46%	2.1	43%
dev. std.			*0.1*		*0.1*	
Ca-biomass	<250 μm		2.1	44%	2.1	44%
dev. std.			*0.1*		*0.1*	

Note: Ø = size particle of biomass; C_0 = initial content P in solution; C_{1h} = P content in solution after 1 h; C_{24h} = P content in solution after 24 h.

Tables 2 and 3 show that P adsorption tests yielded varying outcomes, dependent on the type of Fe-enriched sample and on the solution ($H_2PO_4^-$ or HPO_4^{2-}) employed. The biomass, directly enriched in Fe^{2+} and Fe^{3+}, displayed no capacity to remove either $H_2PO_4^-$ or HPO_4^{2-} ions from the solution. The lack of removal ability was consistent across different contact time (Table 3). In contrast, biomass prepared through double treatment, initially KOH and then $FeSO_4$ or $FeCl_3$, exhibited improved results when exposed to both solutions containing both $H_2PO_4^-$ and HPO_4^{2-} ions. After 1 h, samples treated with KOH and Fe^{2+}, exhibited adsorption of 6% and 14%, respectively, from $H_2PO_4^-$ and HPO_4^{2-} solution, with both reaching about 25% after 24 h. Similarly, samples treated with KOH and Fe^{3+}, after 1 h, adsorbed 26% and 28%, respectively from $H_2PO_4^-$ and HPO_4^{2-} solution, and these values increased to 44% and 37% after 24 h.

3.3. P adsorption kinetics

Based on the collected data regarding the P content in solution at each predetermined time point, it is evident that approximately 48% of P gets adsorbed within the first 15 min after contact. In subsequent samplings, the removal capacity of the Ca-biomass remains almost unchanged, peaking the maximum adsorption of 58% after 24 h. In quantitative terms, 1 g of biomass adsorbs about 1.9 mg of P from the solution after 1 h and this value increases to 2.3 mg of P after 24 h (Fig. 3).

Regarding the study of adsorption kinetics, the physicochemical interaction between the Fe-biomass and P unfolds at a slower pace. Only the Fe^{3+}enriched biomass in the HPO_4^{2-} shows an initial removal rate of just 16% within the first 15 min (Fig. 4).

Data on P uptake rates on biomass were tested with the pseudo-first-order and pseudo-second-order models. Table 4 provides a summary of the parameters derived from the kinetic models applied.

The pseudo-first-order model did not align well our data. In contrast, the pseudo-second-order model effectively characterizes the adsorption mechanisms as indicated by high R^2 values exceeding 0.94. The calculated Q_e compared against the experimental Q_e values further support the model's accuracy. Both the calculated Q_e and K_2 values are consistent with findings reported in the literature [24, 25].

While the experimental data of our samples demonstrated a good fit to the pseudo-second-order model, it's important to consider that the model is grounded in chemisorption theory, which assumes electrons sharing or exchange of between adsorbent and adsorbate, and homogeneity of all adsorption sites. However, this model overlooks the heterogeneous character of the biomass and the existence of other processes such as intraparticle diffusion, mass transfer, or ion interaction. To assess whether intraparticle diffusion is the limiting step, a regression analysis between Q_t and $t^{0.5}$ is usually conducted [26]. The results of this analysis indicated that this model did not align with our experimental data, implying that intraparticle diffusion is not the limiting factor [27]. Thus, the phosphate ion uptake essentially occurs through adsorption on the surfaces of the biomass particles.

3.4. Equilibrium isotherm models

The results of the adsorption studies show a rapid increase in P adsorption by the biomass as the concentration rises, reaching a plateau.

The Langmuir and Freundlich models were applied to the collected data. Among these, the Langmuir isotherm was identified as the most fitting for our data, as shown in Fig. 5. The associated parameters are detailed in Table 5. On the other hand, the Freundlich isotherm was inadequate in describing the adsorption phenomenon. Furthermore, the parameter values of K_f and n ($n > 1$) did not indicate a favourable adsorption intensity.

Table 3
P adsorption from $H_2PO_4^-$ and HPO_4^{2-} solutions.

$H_2PO_4^-$ solution							
Samples	C_0	15′	30′	45′	60′	5 h	24 h
	mgP/50 mL	mg g^{-1}	mg g^{-1}	mg g^{-1}	mg g^{-1}	mg g^{-1}	mg g^{-1}
biomass + KOH + Fe^{2+}	5	<0.1	<0.1	0.2	0.3	0.6	1.2
dev. std.		–	–	*0.3*	*0.2*	*0.1*	*0.2*
% adsorption		<1	<1	4	6	12	24
biomass + KOH + Fe^{3+}	5	0.2	0.9	1.2	1.3	1.8	2.2
dev. std.		*0.1*	*0.1*	*0.1*	*0.1*	*0.1*	*0.1*
% adsorption		4	17	23	26	36	44
HPO_4^{2-} solution							
Samples	C_0 mgP/50 mL	$C_{15'}$ mg g^{-1}	$C_{30'}$ mg g^{-1}	$C_{45'}$ mg g^{-1}	$C_{60'}$ mg g^{-1}	C_{5h} mg g^{-1}	C_{24h} mg g^{-1}
biomass + KOH + Fe^{2+}	5	0.3	0.5	0.6	0.7	0.9	1.3
dev. std.		*0.1*	*0.1*	*0.1*	*0.1*	*0.1*	*0.1*
% adsorption		5	9	12	14	17	27
biomass + KOH + Fe^{3+}	5	0.8	1.1	1.4	1.4	1.7	1.9
dev. std.		*0.1*	*0.2*	*0.1*	*0.2*	*0.2*	*0.2*
% adsorption		16	22	28	28	35	37

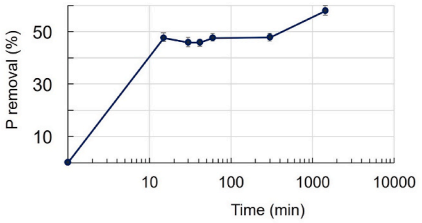

Fig. 3. P adsorption kinetics of Ca-biomass. Based on the data collected on the P content in solution at predetermined time intervals, it is observed that approximately 48% of P is adsorbed within the first 15 min after contact. In subsequent samplings, the removal capacity of the biomass remains almost constant, reaching the maximum adsorption after 24 h with 58% of P adsorbed present in the solution, which is approximately 2.3 mg of P per gram of biomass.

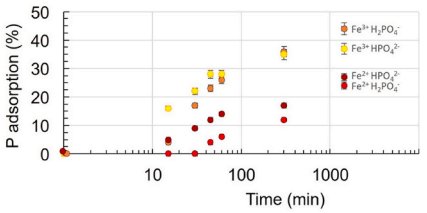

Fig. 4. P adsorption kinetics of Fe-enriched biomass. The physicochemical interaction between the Fe-enriched biomass and P occurs more slowly compared to the calcium-enriched biomass (16% of P removal within the first 15 min only in the biomass samples enriched in Fe^{3+} immersed in the HPO_4^{2-} solution). However, the same biomass removes nearly 40% after 24 h, which is approximately 2.0 mg of P per gram of biomass.

Table 4
Parameters of the applied kinetic models.

Kinetics models	Parameter	Ca-biomass	Fe^{++}-biomass in HPO_4^{2-}	Fe^{+++}-biomass in HPO_4^{2-}	Fe^{++}-biomass in $H_2PO_4^-$	Fe^{+++}-biomass in $H_2PO_4^-$
Pseudo 1st order	Q_e experimental (mg g^{-1})	2.27	1.33	1.87	1.22	2.20
	Qe (mg g^{-1})	1.48	1.02	1.04	1.25	1.67
	K_2 (g μmol^{-1} min^{-1})	37.40	31.99	11.73	38.25	17.26
	R^2	0.15	0.68	0.83	0.85	0.84
Pseudo 2nd order	Qe (mg g^{-1})	2.01	1.24	1.89	1.63	2.24
	K_2 (g μmol^{-1} min^{-1})	13.54	0.93	1.62	0.08	0.52
	R^2	0.96	0.94	0.99	0.97	0.96

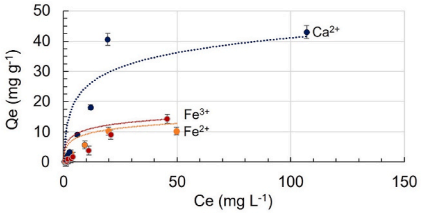

Fig. 5. Langmuir isotherm type for Ca-biomass, Fe^{2+}-biomass and Fe^{3+}-biomass. Adsorption isotherms can be used to predict the adsorption capacity. The collected data were analyzed using both the Langmuir and Freundlich models, which are commonly employed to fit experimental data assuming a monolayer interaction. The figure shows that the Langmuir model, compared to the Freundlich model, provided a better fit to the equilibrium data, and the theoretical maximum adsorption capacities were found to be 54.31 mg of P per gram of biomass.

3.5. The effect of pH values and pH_{pzc}

The mobility of P in variable charge (*v-c*) materials is dominated by the orthophosphate ligand exchange with surface hydroxyl groups on v-c minerals [28]. In our biomass, the zeta potential versus pH curve for the sorbent surface shows slightly negative charge at low pH (<5.0), a strongly negative at higher pH (>6.0) and values close to zero around pH 5.5–5.8. It is widely acknowledged that anions tend to be adsorbed more effectively at pH values lower than pH at PZC, as, during these pH ranges, functional groups on the adsorbent surface are likely to carry a positive net charge [22]. Conversely, when the pH is higher than the pH at PZC the surface

Table 5
Description of fitting parameters applied to Langmuir and Freundlich isotherm models.

Isotherm models	Parameter	Ca-biomass	Fe^{++}- biomass in HPO_4^{2-}	Fe^{+++}- biomass in HPO_4^{2-}
Langmuir	Q_e experimental (mg g^{-1})	42.97	10.23	14.3
	Q_{max} (mg g^{-1})	54.31	14.58	44.21
	K_1 (min^{-1})	0.054	0.067	0.01
	R^2	0.90	0.95	0.99
Freundlich	K_f (min^{-1})	1.67	1.35	0.50
	n	0.45	3.78	1.69
	R^2	0.62	0.56	0.77

charge becomes negative, allowing cations to be adsorbed. As a result, the pH of the medium plays a crucial role in the ion exchange process, directly affecting the P adsorption.

The chemical behaviour of P varies based on the pH of the surrounding environment. At pH below 2.0, it exists as the neutral species H_3PO_4. In aqueous solutions, with pH values ranging from 2.0 to 7.0, it predominantly takes the form of the species H_2PO^{4-}, with a maximum concentration around 3.5 [29]. At pH between 7.0 and 12.0, it is present as HPO_4^{2-}, peaking around 9.0.

Upon contact with untreated biomass, the pH of the $H_2PO_4^-$ solution increased from 5.1 to 5.7 within 1 h, followed by a decrease to 5.3 after 24 h. Initially starting at pH 8.8, the pH of HPO_4^{2-} solution gradually decreased to a sub-acidic pH, upon interaction with the biomass, and eventually stabilized at 5.3. After 1 h and 24 h, the pH of both solutions in contact with the biomass in both situations settled at 5.5, the same pH achieved by immersing the biomass in ultra-pure water.

3.6. The batch experiments desorption

3.6.1. Ca-biomass

When analysing previously enriched biomass, the Ca release measures at 91.6 mg Ca g^{-1}, as opposed to the initially present 143 mg Ca g^{-1}. Notably, the content of firmly bound Ca is about 52 mg Ca g^{-1}, a quantity observed to positively influence the interaction between P and biomass. In contrast, desorption of P from the biomass which was previously used in the initial P adsorption test appears to be minimal. Only 0.2 mg of P g^{-1} was released after the first hour, with this figure increasing to 0.3 mg of P g^{-1} after 24 h. Based on the investigation of adsorption kinetics, it can be deduced that the biomass adsorbed 1.9 mg of P g^{-1} after 1 h and 2.3 mg of P g^{-1} and 24 h. This indicates that about 88% of the P remains securely bound to the biomass.

3.6.2. Fe-biomass

Upon evaluating the Fe release from biomass that was previously enriched in Fe^{2+} and Fe^{3+}, it was found that the released amounts were 0.6 mg of Fe g^{-1} and 3.1 mg of Fe g^{-1}, respectively. This in comparison to the initial presence of 100.2 mg of Fe g^{-1} and 100.5 mg of Fe g^{-1}. Notably, the majority of the Fe content remains firmly bound to the biomass, and this Fe bound content is observed to have a positive influence on the interaction between P and biomass. In contrast, the desorption of P, conducted on the biomass underwent the P adsorption test, is minimal. From Fe^{2+} enriched biomass only 0.15 mg of P g^{-1} was released after the first hour and a similar amount was confirmed after 24 h. Likewise, from Fe^{3+} enriched biomass 0.24 mg of P g^{-1} was released after the first hour, with consistent results after 24 h. Considering the study of adsorption kinetics, the biomass enriched with Fe^{2+} and Fe^{3+} adsorbed 0.3 mg of P g^{-1} and 1.3 mg of P g^{-1} and 0.8 mg of P g^{-1} and 1.9 mg of P g^{-1}, after 1 h and 24 h respectively. This analysis reveals that approximately that about 90% of the P remains securely retained by the biomass.

4. Discussion

4.1. Biomass

4.1.1. Lewis basic sites and PZC

The determination of the Lewis basic sites, representing the count of available complexing sites encompassing both ionic and non-ionic interactions for biomass gram, has been crucial in designing effective adsorption studies involving the enrichment of the biomass with Ca and Fe. The results obtained have shown promise in comparison to other biosorbents used in the literature (biochar [30]), in enhancing the capacity of biomass, through enrichment operations, to uptake negatively charged P ions.

Theorical predictions indicate that the addition of P should influence cation retention in v-c soils [28]. As P adsorption is influenced by both electrostatic attraction and chemical interactions [31,32], it becomes apparent that when the surface of biomass, whether enriched or not, exhibit strong negative charges at pH values greater than 6.0, then P adsorption is hindered due to the increasing electrostatic repulsions with multivalent P anions in the solution. Similarly, for pH values below 5.0, even though the surfaces of biomasses carry only slight negative charges. Hence, these observations suggest that a pH range of about 5.0–6.0 is the potential range for facilitating chemical interaction. The obtained results are explained by the presence in significant amounts of partial or entire negatively charged binding sites on the surface area of our biomass, making difficult any possible P chemical affinity, or any other negatively charged ions. However, it's important to note that a definitive correlation between the P sorption and the zeta potential is

not established. Although surface charge has the potential to influence P sorption, the precise relationship between the two variables is not conclusively determined [33].

4.1.2. Metals

As predicted, the treatment involving KOH followed by 50 mmol of $CaCl_2$, has resulted in the most significant increase in Ca content (Table 1). In terms of Ca, the treatment sequence starting with KOH followed by $FeSO_4$ or $FeCl_3$ exhibits greater effectiveness in binding iron ions onto effectiveness in binding more iron ions onto the biomass (Table 1). This sequence promotes a more significant chemical interaction with Fe^{3+} than with Fe^{2+} ions.

For instance, rock phosphates contain Cd, Co, Cu, Pb and Zn as impurities [34,35]. In the context of fertilisers, Zn, Mn, Co and Pb are generally added to soil. Cu levels are close to the European Union threshold for calcareous soils. Over time, fertiliser application might develop a crop's ability to exclude some heavy metals from the final product, this leads to a reduction in the soil's capacity to transfer these elements. However, elements like As tend to accumulate in grain following fertiliser application [36]. As phosphate rock normally contains heavy metals [37], the use of mineral fertilizers must carefully consider the potential pollution factor. The diverse elemental content observed in the investigated biomass, even at extremely low concentrations, suggests the potential for its direct application in agriculture.

4.2. Batch adsorption performances

The obtained results could be explained because on the surface area of our biomass, partial or entire negatively charged binding sites are present in significant amounts. This abundance of negatively charged sites makes it challenging for any possible P chemical affinity, or any other negatively charged ions. Additionally, the naturally occurring Ca amount in the biomass was insufficient to exert a significant influence on the interaction with phosphate. Considering this, the decision was made to enhance the binding sites on which P could bind by increasing the calcium and iron content in the biomass. The choice of these two ions was closely aligned with our primary objective: to use a natural, or develop a modified, sorbent to apply directly in agriculture practices. This application needed to be achieved without introducing additional substances, and in every case without leaving residues from the modifying treatment that could pollute the soil or cause undesirable effects on plant growth (an example being the use of zirconium as a bridge between natural biomass and phosphate [6]). The Ca-enriched biomass, in contact with $H_2PO_4^-$ fails to establish chemical-physical interaction, which is what happens between Ca and HPO_4^{2-} ions. This outcome might be attributed to the high solubility values of $Ca(H_2PO_4)_2$, which tends to remain in solution rather than bind stably to the biomass surface unlike $CaHPO_4$ (solubility: $CaHPO_4$ 0.1 g L^{-1}, $Ca(H_2PO_4)_2$ 18 g L^{-1}). The Ca increase does influence the P adsorptive capacity which reaches 45% after 1 h, and remains steady after 24 h. This behaviour aligns with the adsorptive capacity of different Ca-enriched biomass [38]. When comparing the behaviour of the four Fe-biomass samples, it becomes evident that the ones treated in KOH and Fe^{2+} have a lower P removal capacity than the samples treated in KOH and Fe^{3+}. Specifically, the samples treated in KOH and Fe^{3+} offer a higher removal capacity manifested as early as 1 h after contact with the two phosphate solutions, but its best performance was obtained in contact with the solution containing $H_2PO_4^-$ ions.

Table 6
Alternative strategies for nutrient recovery of crop residues.

Crop	average P content %	Max P adsorption mg g^{-1}	use	[a]extra treatment	[b]energy	[c]references
cactus pear	0.05		P captor			this paper
		2.1	idem	Ca^{2+}	+	idem
		1.2	idem	Fe^{2+}	+	idem
		2.1	idem	Fe^{3+}	+	idem
almond			soil conditioner	pH	++	25
banana	0.2–0.5	1.0	soil conditioner	compost	+	50–54
clover	0.6		soil conditioner			55
coffee	0.2		growth media			56
hazelnut	0.2		soil conditioner	compost	+	57
orange	0.2		fertiliser			58
palm			fertiliser	temp	++	59
peanut		30	fertiliser	temp, pH	+++	24
potato		190	soil conditioner	pH	+++	60
rice	0.04–0.5	6	soil conditioner	temp	++	30,57,61-65
sugarbeet	0.5		energy, fertiliser	digestion	+++	65
sugarcane	0.01–0.30	250	soil conditioner, irrigation	pH	+++	66–69

[a] Extra treatment, at least one further treatment is required for re-use in agriculture.
[b] Total energy input needed for the specific treatment: + low, ++ medium, +++ high.
[c] References: [22] Faraji et al., 2020; [25] Lim et al., 2012; [50] Kalemelawa et al., 2012; [51] Khatua et al., 2018; [52] Mago et al., 2021; [53] Li et al., 2020; [54] Torma et al., 2018; [55] Ma et al., 2020; [56] Ozdemir et al., 2017; [57] Guerrero et al., 1995; [58] Akinbile et al., 2018; 21 Fang et al., 2020; [59] Quisperima et al., 2022; [60] Xiong et al., 2021; [61] Sharmin et al., 2021; 27 Melia et al., 2019; [62] Pasquali et al., 2018; [63] Wan et al., 2016; [64] Shilpi et al., 2019; [65] Tabinda et al., 2021; [66] Yin et al., 2019; [67] Liao et al., 2022; [68]; Manca et al., 2020[69].

Various biomasses derived from agriculture, whether directly or indirectly, have been used to recover P (Table 6). Some studies have managed to recover even hundreds of milligrams of P per gram of biomass. However, in those cases, the energy input necessary to obtain those results has always been high, and not realistic directly on farm. In comparison to other biomasses, cactus pear has a relatively P adsorption capacity, with an average of 2 mg g^{-1}. Peanut, on the other hand, has a moderate P adsorption capacity with an average of 18 mg g^{-1}. However, peanut is a relatively inexpensive sorbent, making it a good option for some applications. Potato, palm, sugarcane have the highest P adsorption capacities, with an average of <190 mg g^{-1}. However, cactus pear can also be used as a soil conditioner, while palm, sugarcane, and peanut are typically used as fertilizers. This treated biomass is particularly suited for water bodies with low and stable P concentrations. It is not recommended for P recovering from livestock manure.

The total cost of producing a ton of P enriched-cactus pear cladode, possibly loaded with specific cations, packed and distributed varies from 8 to 161 euros. If pruning costs inherent to the crop are also factored in, the total cost becomes 230 euros. These costs are lower than the practical threshold for considering the farm level reuse of P sustainable, which is 320 EUR per tonne [5].

4.3. P adsorption kinetics

The adsorption kinetics (Fig. 3) reveal that the phenomena of chemical-physical interaction between the Ca-enriched cladode and P take place rapidly, with nearly 48% of P removal occurring within the first 15 min. This outcome holds significance considering the implementation of this modified biomass solution to a scale, particularly for treating substantial volumes of water. The relatively short contact time required and resulting swift flows are advantageous factors in this regard. The positive interaction facilitate by the presence of Ca ions is consistent with the findings in other environmental contexts [39], suggesting the simultaneous occurrence of adsorption and co-precipitation phenomena with P.

Equally intriguing are the outcomes obtained with iron ions. Theoretical expectations involve the creation of a coordination bond involving the anionic ligand (Lewis acid-base interaction) in conjunction with electrostatic attraction [40]. Our kinetics patterns (Fig. 4) show a slower and more gradual pattern of adsorption. Over time, the biomasses increase the removal efficiency, reaching, after 24 h, a 44% of P removal in the case of the Fe^{3+}-enriched sample in contact with the solution containing $H_2PO_4^-$ ions. Notably, even in this case, practical application on a real scale holds promise. For instance, a removal of 20% can be achieved after 30–45 min. The adsorption kinetics of Ca- and Fe-treated biomass suggest distinct adsorption times, highlighting very fast mechanisms of biomass-P interactions for Ca-enriched biomass compared to Fe, which exhibits a slower trend. However, there are no major differences in adsorption capacity between the different materials. Consequently, both can provide a good P removal capacity, choosing to use Ca-biomass or Fe-biomass appropriately depending on the application and contact time required.

4.4. Equilibrium isotherm models

The Langmuir model considers a uniform surface with consistent binding energy, and monolayer coverage. Despite their heterogeneous nature, this model has been applied broadly to study the sorption of anions by soils [41,42]. Our kinetic plots for the adsorption of P resamble those described by Zhou et al. [33]. In fact, by simplifying our system, the behaviour of sediments in a body of water is the closest comparison with natural conditions [43]. Both the Langmuir and Freundlich models are used to fit experimental data hypothesizing a monolayer interaction [33]. Our results (Table 5) indicate that the Langmuir model provided a better fit for the equilibrium data, yielding a theoretical maximum adsorption of 54.31 mg g^{-1}. The magnitude of the observed effect surpasses that of similar studies conducted with biological materials [44].

In our system, the adsorption rate showed an increase over time. This phenomenon can be attributed to the abundance of binding sites and a sufficient concentration of P in the solution. As a result, the P immobilization mechanism may involve both instantaneous adsorption (boundary layer diffusion on the external surface) and film diffusion (adsorption on the external surface). Subsequently, the decreased adsorption rate might imply an intraparticle diffusion mechanism as a rate-limiting step [45].

4.5. Desorption performance

The batch desorption experiments were conducted on the enriched biomass to verify the Ca or Fe stability within the adsorbent's chemical composition. Generally, higher desorption values indicate a weaker interaction between adsorbate and adsorbent [46]. Calcium stably bound in the chemical composition of the biomass (52 mg Ca g^{-1}) positively influences the interaction with cladode: 88% of the P is stably retained by the biomass. Similarly, Fe is firmly bound within the chemical composition of the biomass, as less than 3% is released in the desorption test: this results in 90% of the P being retained by the biomass. As a consequence, our attempts to recover P from biomass, and reuse both the P and the biomass itself for new P adsorption cycles from water, proved unsuccessful. This is especially pertinent since, in the soil under oxic environmental conditions, inorganic P in solution would swiftly be adsorbed by intracellular polymeric substances of soil biota and taken up as internal P [47].

Indeed, the P desorption test in HCl required a too-high amount of acid to remove almost all the adsorbed P, or Ca or Fe with phosphate ions. Consequentely, the recovery and reuse of the biomass itself impractical because of the costs of this unsustainable process. These data support the idea of using an agricultural waste product to recover dissolved P in water and replenish both in the soil-plant system. Prioritizing soil health and environmental sustainability, the development of soil conditioners derived from the recycling of waste materials is paramount [48]. The current stage of applicability of this 'novel' material (Ca or Fe-enriched biomass) in real systems, either as a soil conditioner or a plant substrate, is notably uncomplicated and straightforward. This eliminates the need for additional economic investments. This perspective aligns with De-Bashan and Bashan [49] who suggest the use of filter that

effectively traps P and, once saturated, reused as fertiliser. The pruning residues of the cactus pear are also used directly as a soil conditioner in traditional agronomic practice. Our findings underscore that a low energy impact treatment, which can be performed on farm, can increase its value in terms of biogeochemical cycles useful for cultivated plants. This is particularly relevant as cladodes themselves possess minimal P content.

The transferability of findings from synthetic solutions to real-world scenarios with complex wastewater compositions should be further investigated to assess the applicability under real environmental conditions. The lack of comprehensive validation experiments hinders the assessment of the technique's practical feasibility, efficiency, and potential limitations. Future approaches should pivot from perceiving waste as a problem to recognizing it as a surplus [70]. This shift emphasizes the significance of transition mediators in bringing together diverse stakeholders' perspectives to facilitate local transitions.

5. Conclusions

Dried, ground, and calcium or iron enriched pruning wastes *Opuntia ficus-indica* have been successfully applied as an environmentally friendly and efficient adsorbent for P removing from artificially enriched aqueous solutions. The maximum P adsorption capacities obtained from Ca-cladode, Fe^{2+}-cladode and Fe^{3+}-cladode were 2.16 ± 0.02 mg g^{-1}, 1.3 ± 0.16 and 2.0 ± 0.3, respectively. Experimental data on P adsorption were represented by Langmuir isotherm models.

The distinctive behaviour exhibited by cladodes loaded with Ca and Fe, particularly ferric iron, suggests a treatment that is easily implementable even at farm level. This presents intriguing possibilities for other biomasses as well, expanding the scientific horizon. The insights gained from desorption studies was important in supporting the original idea behind this work: utilising agricultural waste products to recover dissolved P from water and reintegrate it into the soil-plant system. Given the current stage of development, the application of this 'novel' material in a real system, whether as soil conditioner or plant substrate, at this point, can be fairly straightforward and uncomplicated, without necessitating additional economic investment.

Author contribution statement

Conceived and designed the experiments, Filippo Saiano, and Riccardo Scalenghe; Performed the experiments, Nicolò Auteri. Analyzed and interpreted the data, Nicolò Auteri, Filippo Saiano, and Riccardo Scalenghe; - Contributed reagents, materials, analysis tools or data, Filippo Saiano, and Riccardo Scalenghe; - Wrote the paper, Nicolò Auteri, Filippo Saiano, and Riccardo Scalenghe.

Data availability statement

Data is provided both within the article itself and in the supplementary material..

Declaration of competing interest

The authors declare that they have no known competing financial interests or personal relationships that could have appeared to influence the work reported in this paper.

Acknowledgements

We are deeply indebted to Marco Prati of the University of Turin for the electrophoretic mobility measurements, and for his friendship. We are grateful to the editor and the anonymous reviewers for their insightful advice, which has undoubtedly improved the manuscript.

Appendix A. Supplementary data

Supplementary data to this article can be found online at https://doi.org/10.1016/j.heliyon.2023.e19996.

References

[1] C. Weissert, J. Kehr, Macronutrient Sensing and Signaling in Plants, Plant Macronutrient Use Efficiency, 2018, pp. 45–64, https://doi.org/10.1016/B978-0-12-811308-0.00003-X.
[2] B. Li, K.B. Bicknell, A. Renwick, Peak phosphorus, demand trends and implications for the sustainable management of phosphorus in China, Resour. Conserv. Recycl. 146 (2019) 316–328, https://doi.org/10.1016/j.resconrec.2019.03.033.
[3] B. Zhou, Y. Xu, R.D. Vogt, X. Lu, X. Li, X. Deng, A. Yue, L. Zhu, Effects of land use change on phosphorus levels in surface waters—a case study of a watershed strongly influenced by agriculture, Water Air Soil Pollut. 227 (5) (2016) 160, https://doi.org/10.1007/s11270-016-2855-6.
[4] G. Pan, T. Lyu, R. Mortimer, Comment: closing phosphorus cycle from natural waters: Re-capturing phosphorus through an integrated water-energy-food strategy, J. Environ. Sci. (2018), https://doi.org/10.1016/j.jes.2018.02.018.
[5] N. Auteri, F. Saiano, R. Scalenghe, Recycling phosphorus from agricultural streams: grey and green solutions, Agronomy 12 (2022) 2938, https://doi.org/10.3390/agronomy12122938.

[6] Y. Jiang, Y. Chen, Q. Du, J. Shi, Adsorption of different forms of phosphorus on modified corn bracts, Water Environ. Res. 91 (2019) 748–755, https://doi.org/10.1002/wer.1105.

[7] H.A.T. Banu, P. Karthikeyan, S. Meenakshi, Comparative studies on revival of nitrate and phosphate ions using quaternized corn husk and jackfruit peel, Bioresour. Technol. Rep. 8 (2019), 100331, https://doi.org/10.1016/j.biteb.2019.100331.

[8] Y. Shang, K. Guo, P. Jiang, X. Xu, B. Gao, Adsorption of phosphate by the cellulose-based biomaterial and its sustained release of laden phosphate in aqueous solution and soil, Int. J. Biol. Macromol. 109 (2018) 524–534, https://doi.org/10.1016/j.ijbiomac.2017.12.118.

[9] X. Xu, B. Gao, W. Wang, Q. Yue, Y. Wang, S. Ni, Adsorption of phosphate from aqueous solutions onto modified wheat residue: characteristics, kinetic and column studies, Colloids Surf. B Biointerfaces 70 (2009) 46–52, https://doi.org/10.1016/j.colsurfb.2008.12.006.

[10] H. Nouri, A. Abdedayem, I. Hamidi, S.S. Najjar, A. Ouederni, Biosorption of lead heavy metal on prickly pear cactus biomaterial: kinetic, thermodynamic and regeneration studies, Cellul. Chem. Technol. 55 (2021) 919–932.

[11] R. Aziam, L. Boukarma, A. Zaghloul, R. Benhiti, E. Eddaoudi, M. Zerbet, M. Chiban, Factor design methodology for modelling and optimization of carcinogenic acid dye ad-sorption onto Moroccan prickly pear cactus peel, E3S Web Conf. 240 (2021), 02005, https://doi.org/10.1051/e3sconf/202124002005.

[12] Enea, Valorizzazione di risorse biologiche da *Opuntia ficus-indica*, 2017. https://www.enea.it/it/seguici/events/italiamex/2BacchettaWORKSHOP_2017.pdf.

[13] F. Saiano, M. Ciofalo, S.O. Cacciola, S. Ramirez, Metal ion adsorption by *Phomopsis* sp. biomaterial in laboratory experiments and real wastewater treatments, Water Res. 39 (2005) 2273–2280, https://doi.org/10.1016/j.watres.2005.04.022.

[14] M. Barbera, S. Indelicato, D. Bongiorno, V. Censi, F. Saiano, D. Piazzese, Untreated Opuntia ficus indica for the efficient adsorption of Ni(II), Pb(II), Cu(II) and Cd(II) ions from water, Molecules 28 (2023) 3953, https://doi.org/10.3390/molecules28093953.

[15] T. Bellini, D. Degiorgio, F. Mantegazza, F. Ajmone Marsan, C. Scarnecchia, Electrokinetic properties of colloids of variable charge. I. Electrophoretic and electro-optic characterization, J. Chem. Phys. 103 (1995) 8228, https://doi.org/10.1063/1.470187.

[16] R.W. O'Brien, L.R. White, Electrophoretic mobility of a spherical colloidal particle, J. Chem. Soc., Faraday Trans. 2 74 (1978) 1607–1626, https://doi.org/10.1039/F29787401607.

[17] Y. Ho, G. McKay, Pseudo-second-order model for sorption process, Process Biochem. 34 (1999) 451–465.

[18] Y. Ho, J. Ng, G. McKay, Kinetics of pollutants sorption by biosorbents: review, Separ. Purif. Methods 29 (2000) 189–232.

[19] M. Quintero-García, E. Gutiérrez-Cortez, M. Bah, A. Rojas-Molina, M.d.l.A. Cornejo-Villegas, A. Del Real, I. Rojas-Molina, Comparative analysis of the chemical composition and physicochemical properties of the mucilage extracted from fresh and dehydrated *Opuntia ficus-indica* cladodes, Foods 10 (2021) 2137, https://doi.org/10.3390/foods10092137.

[20] T. Hong, J.Y. Yin, S.P. Nie, M.Y. Xie, Applications of infrared spectroscopy in polysaccharide structural analysis: progress, challenge and perspective, Food Chem. 12 (2021), 100168, https://doi.org/10.1016/j.fochx.2021.100168.

[21] S. Barsberg, Prediction of vibrational spectra of polysaccharides-simulated IR spectrum of cellulose based on density functional theory (DFT), J. Phys. Chem. B 114 (36) (2010), https://doi.org/10.1021/jp104213z, 11703 117011708.

[22] T.S. Anirudhan, S. Rijith, L. Divya, Preparation and application of a novel functionalized coconut coir pith as a recyclable adsorbent for phosphate removal, Separ. Sci. Technol. 44 (2009) 2774–2796, https://doi.org/10.1080/01496390903017899.

[23] A. Sowmya, S. Meenakshi, Effective removal of nitrate and phosphate anions from aqueous solutions using functionalized chitosan beads, Desalination Water Treat. 52 (13–15) (2014) 2583–2593, https://doi.org/10.1080/19443994.2013.798842.

[24] L. Fang, J. Li, S. Donatello, C.R. Cheeseman, C.S. Poon, D.C.W. Tsang, Use of Mg/Ca modified biochars to take up phosphorus from acid-extract of incinerated sewage sludge ash (ISSA) for fertilizer application, J. Clean. Prod. 244 (2020), 118853, https://doi.org/10.1016/j.jclepro.2019.118853.

[25] B. Faraji, M. Zarabi, Z. Kolahchi, Phosphorus removal from aqueous solution using modified walnut and almond wooden shell and recycling as soil amendment, Environ. Monit. Assess. 192 (2020) 373, https://doi.org/10.1007/s10661-020-08326-x.

[26] Ginestra, G., M.L. Parker, R.N. Bennett, J. Robertson, G. Mandalari, A. Narbad, R.B. Lo Curto, G. Bisignano, C.B. Faulds, K.W. Waldron, Anatomical, chemical, and biochemical characterization of cladodes from prickly pear [*Opuntia ficus-indica* (L.) Mill.], J. Agric. Food Chem. 57 (2009), 10323–10330.

[27] T. Nharingo, M. Moyo, Application of *Opuntia ficus-indica* in bioremediation of wastewaters. A critical review, J. Environ. Manage. 166 (2016) 55–72, https://doi.org/10.1016/j.jenvman.2015.10.005.

[28] P. Sollins, G.P. Robertson, G. Uehara, Nutrient mobility in variable- and permanent-charge soils, Biogeochemistry 6 (3) (1988) 181–199, https://doi.org/10.1007/BF02182995.

[29] M. Aryal, M. Liakopoulou-Kyriakides, Equilibrium, kinetics and thermodynamic studies on phosphate biosorption from aqueous solutions by Fe(III)-treated *Staphylococus xylosus* biomass: common ion effect, Colloids Surf. A Physicochem. Eng. Asp. 387 (1) (2011) 43–49, https://doi.org/10.1016/j.colsurfa.2011.07.019.

[30] P.M. Melia, R. Busquets, P.S. Hooda, A.B. Cundy, S.P. Sohi, Driving forces and barriers in the removal of phosphorus from water using crop residue, wood and sewage sludge derived biochars, Sci. Total Environ. 675 (2019) 623–631, https://doi.org/10.1016/j.scitotenv.2019.04.232.

[31] M. Ozacar, I.A. Sengil, Adsorption of reactive dyes on calcined alunite from aqueous solutions, J. Hazard Mater. B98 (2003) 211–224, https://doi.org/10.1016/S0304-3894(02)00358-8.

[32] L. Yan, J. Wang, X. Han, Y. Ren, Q. Liu, F. Li, Enhanced microwave absorption of Fe nanoflakes after coating with SiO_2, Nanotechnology 21 (2010), 095708, https://doi.org/10.1088/0957-4484/21/9/095708.

[33] A. Zhou, H. Tang, D. Wang, Phosphorus adsorption on natural sediments: modeling and effects of pH and sediment composition, Water Res. 39 (2005) 1245–1254, https://doi.org/10.1016/j.watres.2005.01.026.

[34] L.G. De López Camelo, S.R. De Miguez, L. Marbán, Heavy metals input with phosphate fertilizers used in Argentina, Sci. Total Environ. 204 (3) (1997) 245–250, https://doi.org/10.1016/S0048-9697(97)00187-3.

[35] Sabiha-Javied, T. Mehmood, M.M. Chaudhry, M. Tufail, N. Irfan, Heavy metal pollution from phosphate rock used for the production of fertilizer in Pakistan, Microchem. J. 91 (1) (2009) 94–99, https://doi.org/10.1016/j.microc.2008.08.009.

[36] X.-X. Chen, Y.-M. Liu, Q.-Y. Zhao, X.-P. Cao W.-Q., Chen, C.-Q. Zou, Health risk assessment associated with heavy metal accumulation in wheat after long-term phosphorus fertilizer application, Environ. Pollut. 262 (2020), 114348, https://doi.org/10.1016/j.envpol.2020.114348.

[37] R.W. Scholz, A.E. Ulrich, M. Eilittä, A. Roy, Sustainable use of phosphorus: a finite resource, Sci. Total Environ. 461–462 (2013) 799–803.

[38] S. Wang, L. Kong, J. Long, M.Z. Su, X. Chang, D. Chen, G. Song, K. Shih, Adsorption of phosphorus by calcium-flour biochar: isotherm, kinetic and transformation studies, Chemosphere 195 (2018) 666–672, https://doi.org/10.1016/j.chemosphere.2017.12.101.

[39] C.A. Arias, M. Del Bubba, H. Brix, Phosphorus removal by sands for use as media in subsurface flow constructed reed beds, Water Res. 35 (5) (2001) 1159–1168, https://doi.org/10.1016/S0043-1354(00)00368-7.

[40] S. Sengupta, A. Pandit, Selective removal of phosphorus from wastewater combined with its recovery as a solid-phase fertilizer, Water Res. 45 (11) (2011) 3318–3330, https://doi.org/10.1016/j.watres.2011.03.044.

[41] W.A. House, F.H. Denison, Factors influencing the measurement of equilibrium phosphate concentrations in river sediments, Water Res. 34 (2000) 1187–1200, https://doi.org/10.1016/S0043-1354(99)00249-3.

[42] D.M. Bubba, C.A. Arias, H. Brix, Phosphorus adsorption maximum of sands for use as media in subsurface flow constructed reed beds as measured by the Langmuir isotherm, Water Res. 37 (2003) 3390–3400, https://doi.org/10.1016/S0043-1354(03)00231-8.

[43] Q. Wang, Y. Li, Phosphorus adsorption and desorption behavior on sediments of different origins, J. Soils Sediments 10 (6) (2010) 1159–1173, https://doi.org/10.1007/s11368-010-0211-9.

[44] W. Pan, H. Xie, Y. Zhou, Q. Wu, J. Zhou, X. Guo, Simultaneous adsorption removal of organic and inorganic phosphorus from discharged circulating cooling water on biochar derived from agricultural waste, J. Clean. Prod. 383 (2023), 135496, https://doi.org/10.1016/j.jclepro.2022.135496.

[45] D. Zhu, Y. Chen, H. Yang, S. Wang, X. Wang, S. Zhang, H. Chen, Synthesis and characterization of magnesium oxide nanoparticle-containing biochar composites for efficient phosphorus removal from aqueous solution, Chemosphere 247 (2020), 125847, https://doi.org/10.1016/j.chemosphere.2020.125847.

[46] B.O. Nardis, J.R. Franca, J.S.D.S. Carneiro, J. Ribeiro Soares, L.R. Guimarães Guilherme, C.A. Silva, L.C.A. Melo, Production of engineered-biochar under different pyrolysis conditions for phosphorus removal from aqueous solution, Sci. Total Environ. 816 (2022), 151559, https://doi.org/10.1016/j.scitotenv.2021.151559.
[47] Y. Zhou, B.T. Nguyen, C. Zhou, L. Straka, Y.S. Lai, S. Xia, B.E. Rittmann, The distribution of phosphorus and its transformations during batch growth of *Synechocystis*, Water Res. 122 (2017) 355–362, https://doi.org/10.1016/j.watres.2017.06.017.
[48] Y. Zhao, Y. Li, F. Yang, Critical review on soil phosphorus migration and transformation under freezing-thawing cycles and typical regulatory measurements, Sci. Total Environ. 751 (2021), 141614, https://doi.org/10.1016/j.scitotenv.2020.141614.
[49] L.E. De-Bashan, Y. Bashan, Recent advances in removing phosphorus from wastewater and its future use as fertilizer (1997-2003), Water Res. 38 (19) (2004) 4222–4246, https://doi.org/10.1016/j.watres.2004.07.014.
[50] S.L. Lim, T.Y. Wu, E.Y.S. Sim, P.N. Lim, C. Clarke, Biotransformation of rice husk into organic fertilizer through vermicomposting, Ecol. Eng. 41 (2012) 60–64, https://doi.org/10.1016/j.ecoleng.2012.01.011.
[51] F. Kalemelawa, E. Nishihara, T. Endo, Z. Ahmad, R. Yeasmin, M.M. Tenywa, S. Yamamoto, An evaluation of aerobic and anaerobic composting of banana peels treated with different inoculums for soil nutrient replenishment, Bioresour. Technol. 126 (2012) 375–382, https://doi.org/10.1016/j.biortech.2012.04.030.
[52] C. Khatua, S. Sengupta, V.K. Balla, B. Kundu, A. Chakraborti, S. Tripathi, Dynamics of organic matter decomposition during vermicomposting of banana stem waste using *Eisenia fetida*, Waste Manage. 79 (2018) 287–295, https://doi.org/10.1016/j.wasman.2018.07.043.
[53] M. Mago, A. Yadav, R. Gupta, V.K. Garg, Management of banana crop waste biomass using vermicomposting technology, Bioresour. Technol. 326 (2021), 124742, https://doi.org/10.1016/j.biortech.2021.124742.
[54] W. Li, S.A. Bhat, J. Li, G. Cui, Y. Wei, T. Yamada, F. Li, Effect of excess activated sludge on vermicomposting of fruit and vegetable waste by using novel vermireactor, Bioresour. Technol. 302 (2020), 122816, https://doi.org/10.1016/j.biortech.2020.122816.
[55] S. Torma, J. Vilček, T. Lošák, S. Kužel, A. Martensson, Residual plant nutrients in crop residues – an important resource, Acta Agric. Scand. B 68 (2018) 358–366, https://doi.org/10.1080/09064710.2017.1406134.
[56] N.L. Ma, S.C. Khoo, W. Peng, C.M. Ng, C.H. Teh, Y.K. Park, S.S. Lam, Green application and toxic risk of used diaper and food waste as growth substitute for sustainable cultivation of oyster mushroom (*Pleurotus ostreatus*), J. Clean. Prod. 268 (2020), 122272, https://doi.org/10.1016/j.jclepro.2020.122272.
[57] S. Ozdemir, O.H. Dede, M. Yaqub, Assessment of long-term nutrient effective waste-derived growth media for ornamental nurseries, Waste Biomass Valori. 8 (2017) 2663–2671, https://doi.org/10.1007/s12649-016-9716-9.
[58] C.C. Guerrero, J.C. de Brito, N. Lapa, J.F.S. Oliveira, Re-use of industrial orange wastes as organic fertilizers, Bioresour. Technol. 53 (1995) 43–51, https://doi.org/10.1016/0960-8524(95)00050-O.
[59] C.O. Akinbile, B.T. Ikuomola, O.O. Olanrewaju, T.E. Babalola, Assessing the efficacy of *Azolla pinnata* in four different wastewater treatment for agricultural re-use: a case history, Sust. Water Res. Manage. 5 (2019) 1009–1015, https://doi.org/10.1007/s40899-018-0273-1.
[60] A. Quisperima, S. Pérez, E. Flórez, N. Acelas, Valorization of potato peels and eggshells wastes: Ca-biocomposite to remove and recover phosphorus from domestic wastewater, Bioresour. Technol. 343 (2022), 126106, https://doi.org/10.1016/j.biortech.2021.126106.
[61] Q. Xiong, X. Wu, H. Lv, S. Liu, H. Hou, X. Wu, Influence of rice husk addition on phosphorus fractions and heavy metals risk of biochar derived from sewage sludge, Chemosphere 280 (2021), 130566, https://doi.org/10.1016/j.chemosphere.2021.130566.
[62] N. Sharmin, D.A. Sabatini, E.C. Butler, Phosphorus recovery and reuse using calcium-silicate hydrate made from rice husk, J. Environ. Chem. Eng. 147 (2021), 04021015. https://ascelibrary.org/doi/10.1061/%28ASCE%29EE.1943-7870.0001877.
[63] M. Pasquali, A. Zanoletti, L. Benassi, S. Federici, L.E. Depero, E. Bontempi, Stabilized biomass ash as a sustainable substitute for commercial P-fertilizers, Land Degrad. Dev. 29 (2018) 2199–2207, https://doi.org/10.1002/ldr.2915.
[64] J. Wan, X. Liu, C. Wu, Y. Wu, Nutrient capture and recycling by periphyton attached to modified agrowaste carriers, Environ. Sci. Pollut. Res. 23 (2016) 8035–8043, https://doi.org/10.1007/s11356-015-5988-z.
[65] S. Shilpi, D. Lamb, N. Bolan, B. Seshadri, G. Choppala, R. Naidu, Waste to Watt: anaerobic digestion of wastewater irrigated biomass for energy and functional production, J. Environ. Manage. 239 (2019) 73–83, https://doi.org/10.1016/j.jenvman.2019.02.122.
[66] A.B. Tabinda, U. Fatima, M. Batool, A. Yasar, R. Rasheed, A. Iqbal, Y. Mahfooz, A study on recycling and reuse of sugar mill industrial waste, Energy Sources A 43 (2021) 1759–1768, https://doi.org/10.1080/15567036.2019.1647311.
[67] J. Yin, C.B. Deng, X.F. Wang, G. Chen, V.G. Mihucz, P.G. Xu, Q.C. Deng, Effects of long-term application of vinasse on physicochemical properties, heavy metals content and microbial diversity in sugarcane field soil, Sugar Technol. 21 (2019) 62–70, https://doi.org/10.1007/s12355-018-0630-2.
[68] Y. Liao, S. Chen, Q. Zheng, B. Huang, J. Zhang, H. Fu, H. Gao, Removal and recovery of phosphorus from solution by bifunctional biochar, Inorg. Chem. Commun. 139 (2022), 109341, https://doi.org/10.1016/j.inoche.2022.109341.
[69] A. Manca, M.R. da Silva, I.A. Guerrini, D.M. Fernandes, R.L. Villas Bôas, L.C. da Silva, A.C. da Fonseca, M.C. Ruggiu, C.V. Cruz, D.C.L. Sivisaca, C.M.A. Mateus, I. Murgia, E. Grilli, A. Ganga, G.F. Capra, Composted sewage sludge with sugarcane bagasse as a commercial substrate for *Eucalyptus urograndis* seedling production, J. Clean. Prod. 269 (2020), 122145, https://doi.org/10.1016/j.jclepro.2020.122145.
[70] M. Hassan Awad, Microfoundations of the waste-to-resource problem in circular economy transitions: antenarratives of phosphorus in Dutch agribusiness (2008–2014), J. Clean. Prod. 406 (2023), 136952, https://doi.org/10.1016/j.jclepro.2023.136952.